Microstructure of dispersions of lamellar droplets carrying anchoring hydrophobically endcapped poly(sodium acrylate)s as novel steric stabilizers

Kevelam, J; Martinucci, S.; Engberts, J.B.F.N.; Blokzijl, W.; van de Pas, J.C.; Blonk, H.; Versluis, P.; Visser, Antonie J.W.G.

Published in:
Langmuir

DOI:
10.1021/la981636v

Microstructure of Dispersions of Lamellar Droplets Carrying Anchoring Hydrophobically Endcapped Poly(sodium acrylate)s as Novel Steric Stabilizers

Jan Kevelam, Silvia Martinucci, and Jan B. F. N. Engberts*

Department of Organic and Molecular Inorganic Chemistry, University of Groningen, Nijenborgh 4, 9747 AG Groningen, The Netherlands

Wilfried Blokzijl, John van de Pas, Han Blonk, and Peter Versluis

Unilever Research Vlaardingen, Olivier van Noortlaan 120, 3133 AT Vlaardingen, The Netherlands

Antonie J. W. G. Visser

Microspectroscopy Centre, Department of Biomolecular Sciences, Wageningen Agricultural University, Dreijenlaan 3, 6703 HA Wageningen, The Netherlands

Received November 24, 1998. In Final Form: April 26, 1999

We have studied the influence of anchoring hydrophobically single-endcapped poly(sodium acrylate)s on the microstructure and colloidal stabilization of self-assembled lamellar droplets formed from a mixture of anionic and nonionic surfactants in concentrated aqueous electrolyte solutions. A fluorescently labeled hydrophobically endcapped poly(sodium acrylate) has been synthesized and characterized using time-resolved fluorescence spectroscopic techniques; it appears that the fluorophore has considerable freedom of internal rotation. Using this labeled poly(sodium acrylate), the presence of an adsorbed polymer layer bound to the surface of the droplets was imaged by confocal scanning laser microscopy, providing visual evidence that the droplets are sterically stabilized. Laser diffraction and refractive index measurements were employed to determine average particle sizes of the colloidal particles, and it was established that increasing the molecular weight of the hydrophilic (pendant) backbone at a constant (hydrophobic) anchor density, or increasing the concentration of polymer in the dispersion at constant molecular weight, results in a decrease of the average droplet size. This is in agreement with theoretical predictions that an increased lateral pressure in the adsorbed layer, due to a higher polymer segment density near the surface, is relieved by increasing the curvature of the lamellar droplets. Finally, the adsorption of hydrophobically endcapped polymers to lamellar droplets has been described in terms of a Freundlich isotherm, reflecting the degressive increase of the amount of polymer adsorbed onto the surface of the droplets with increasing polymer concentration. Again, an increase of lateral pressure with surface coverage is held responsible for this effect.

Introduction

Colloidal dispersions are widely encountered in the chemical industry, comprising inks, paints, ceramics, detergents and so on.[1] A fundamental problem is to control the intrinsic tendency of the colloidal particles to flocculate due to strong (van der Waals) attractions. Colloidal stability is often attained by the attachment of polymers to the particles. In good solvents, the polymers avoid each other and, provided that the repulsive forces have a longer range than the dispersion forces, the particles will be kept apart. This mechanism is called steric stabilization.[2]

Colloidal dispersions of solid particles covered by irreversibly attached polymer chains are well understood theoretically. The repulsive forces between sparsely grafted polymer layers ("mushrooms") are primarily of entropic origin and are related to the configuration changes of the coils upon close approach. In the opposite ("brush") regime, extended polymer chains repel each other as the surface-to-surface distance between the particles approaches twice the adsorbed layer thickness. The repulsion results from an osmotic flow of solvent into this overlap region. From another point of view, the increase of osmotic forces is due to monomer-excluded volume interactions. These qualitative arguments can be translated into force−distance curves or potential energy diagrams using mean-field,[3] scaling,[4] or self-consistent field[5] calculations. Moreover, these models may be verified experimentally by directly measuring the forces between grafted surfaces using the Israelachvili surface force apparatus.[6]

With the advent of Stealth liposomes[7] in biomedical applications, where steric stabilization is employed to increase the circulation time in the body of PEG-coated vesicles,[8] the understanding of steric stabilization of flexible, deformable surfaces such as bilayer membranes

(1) (a) Russel, W. B.; Saville, D. A.; Schowalter, W. R. *Colloidal Dispersions*; Cambridge University Press: Cambridge, 1989. (b) Proceedings of the 37th General Meeting of the German Colloid Society, *Interfaces, Surfactants and Colloids in Engineering*, Dresden, Germany, Sept. 26−29; *Prog. Colloid Polym. Sci.* **1996**, *101*, 1.

(2) Napper, D. H. *Polymeric Stabilization of Dispersions*; Academic Press: London, 1983.

(3) Milner, S. T. *Europhys. Lett.* **1988**, *7*, 695.

(4) De Gennes, P.-G. *Macromolecules* **1980**, *13*, 1069.

(5) Zhulina, E. B.; Borisov, O. V.; Pryamitsyn, V. A. *J. Colloid Interface Sci.* **1990**, *137*, 495.

(6) Hadziioannou, G.; Patel, S.; Grannick, S.; Tirrell, M. *J. Am. Chem. Soc.* **1986**, *108*, 2871.

(7) Registered trademark from Liposome Technology, Inc.; cf. Lasic, D. D. *Polym. Prepr.* **1997**, *38*, 543.

10.1021/la981636v CCC: $18.00
Published on Web 06/19/1999

Scheme 1

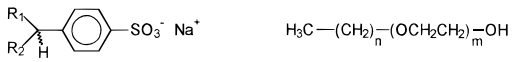

NaDoBS
<R_1> = $C_{3.1}$, <R_2> = $C_{7.2}$

$C_{13\text{-}15}EO_{<7>}$
n = 12-14, <m> = 7

has gained increasing importance. This is equally true with regard to the formulation of certain structured liquid laundry detergents, containing salted-out surfactants (vide infra): a concentrated dispersion of multilamellar vesicles is colloidally stabilized by the addition of an anchoring polymer.[9,16] The present study provides further technological insights required for this purpose.

The multilamellar vesicles that are employed in this study are formed from a mixture of single-tailed anionic (sodium dodecylbenzenesulfonate, NaDoBS) and nonionic ($C_{13-15}EO_{\langle 7\rangle}$) surfactants (see Scheme 1 and Experimental Section for details).[9] When dissolved in pure water at sufficiently high concentrations, mixed micelles will be formed since the geometric packing parameter[10] is lower than 0.5. However, since a salting-out electrolyte is present (trisodium citrate, NaCit), a lamellar phase is formed, because the size of the nonionic surfactant headgroup is reduced through dehydration, and the charge repulsion between the anionic surfactant headgroups is diminished through increased counterion binding. The overall result is a decrease of the optimal cross-sectional headgroup surface area at constant hydrophobic tail length, so that the packing parameter increases and the formation of a lamellar phase is favored.

When the dispersion is viewed under a light microscope, with crossed polarizers, Maltese crosses are observed, indicating that spherical multilamellar droplets are present.[11] We mention two important reasons why a lamellar dispersion is formed instead of a continuous lamellar phase. (1) The surfactants are of a technical grade, so that they comprise a broad distribution of surfactant molecular architectures. This allows the bilayers to be curved due to a possible asymmetric distribution of the surfactant molecules in the bilayer.[12] (2) The surfactants−water−salt mixture is prepared under shear. Mechanical agitation promotes the formation of curved rather than flat bilayer structures. However, a continuous lamellar phase is not observed even after standing for a long time (>1 year), which provides strong indications that a lamellar dispersion is the thermodynamically favored state.

Another consequence of the high electrolyte concentration and the concomitant poor solvency of the nonionic headgroups is that the lamellar droplets will flocculate. The osmotic interactions between nonionic headgroups change from repulsive to attractive above a threshold electrolyte concentration. The system under investigation phase-separates within minutes to form an isotropic continuous phase containing only water and 30% (w/w) NaCit as well as a lamellar, surfactant-rich phase of lower density. To stabilize the colloidal dispersion, random copolymers of lauryl methacrylate and sodium acrylate have been added as steric stabilizers. Presumably, the dodecyl groups of the copolymer are anchored into the outer bilayer of the lamellar droplets, while the pendant hydrophilic backbones are responsible for the repulsive interlamellar forces.

The aim of this study is first of all to obtain insights into the general principles governing steric stabilization of self-assembled deformable bilayer membranes. In particular, we wish to answer the following questions: (1) Are the polymers irreversibly grafted to the bilayer membranes, or are they involved in an adsorption equilibrium? (2) Do anchored polymers affect the size or shape of the (multilamellar) vesicles? And if so, what is the role of the molecular weight of the polymer? (3) Are the average droplet size and the amount of adsorbed polymer interdependent, and can we understand and predict any relationships between these parameters?

Of practical importance is our aim to understand in greater detail colloidal stabilization of lamellar droplets in liquid detergent formulations.

Experimental Section

Materials. *1. Synthesis of Hydrophobically Single-Endcapped Poly(sodium acrylate)*s. Single-endcapped hydrophobically modified poly(sodium acrylate)s of molecular weight exceeding ca. 3000 were synthesized using a hydrophobic initiator in 1,4-dioxane (solution polymerization) or methyl ethyl ketone (precipitation polymerization). The following example illustrates the general procedure:

A 250 mL round-bottomed flask was loaded with 5 g (69.4 mmol) of freshly distilled acrylic acid (Janssen, 99%), 50 mL of 1,4-dioxane (Merck, pro analysi) and 0.57 g (1.33 mmol) of dilauroyl peroxide (Aldrich). The flask was connected to a reflux condenser fitted with a $CaCl_2$ tube and was heated on an oil bath at 80 °C with stirring. The reaction mixture was kept at this temperature overnight. After cooling to room temperature, the clear, slightly viscous solution was precipitated in 300 mL of pentane to remove most of the 1,4-dioxane. The viscous precipitate was dissolved in dry methanol. The methanolic solution was slowly added to a stirred solution of 3.6 g (66.7 mmol) of sodium methoxide (Merck) in 100 mL of dry methanol. A white solid precipitated, which was filtered off under reduced pressure. The crude product was dried in vacuo at 30 °C to remove most of the remaining 1,4-dioxane and methanol. The polymer was dissolved in water to obtain a solution of about 5−10% (w/w). The polymer was neutralized by adding sodium hydroxide until pH 9, and the solution was freeze-dried. To remove the last traces of solvent, the polymer was finely powdered and dried at 60 °C over P_2O_5 in vacuo for at least 2 h. The isolated yield was 70% or higher.

Polymers with a molecular weight exceeding 3000−8000 can be obtained using lower relative amounts of initiator and by performing the reaction under a nitrogen atmosphere. The fraction of initiator radical fragments

(8) Blume, G.; Cevc, G. *Biochim. Biophys. Acta* **1990**, *102*, 91. (b) Needham, D.; McIntosh, T. J.; Lasic, D. D. *Biochim. Biophys. Acta* **1992**, 1108, 40.

(9) Van de Pas, J. C. Ph.D. Thesis, University of Groningen, Groningen, The Netherlands, 1993.

(10) Israelachvili, J. N.; Mitchell, D.; Ninham, R. W. *J. Chem. Soc., Faraday Trans. 1* **1976**, *72*, 1525.

(11) Larson, K. *Z. Phys. Chem.* **1967**, *56*, 173.

(12) Safran, S. A.; Pincus, P.; Andelman, D. A. *Science* **1990**, *248*, 354.

(13) The degree of polymerization (DP) can be related to the concentrations of chain transfer agent (RSH), initiator (IN), and acrylic acid (AA) according to the following equation, which is based upon a polymerization scheme in which all termination reactions occur such that single-endcapped products are formed: $1/DP = k[RSH]/[AA] + 2k^*[IN]/[AA]$. k is the chain transfer constant (−0.4 for $C_{12}H_{25}SH$ under the experimental conditions) and k^* denotes the efficiency of initiation (i.e., $k^* = 0.10-0.26$). This equation is similar to the general equation for chain transfer as proposed previously (Mayo, F. R *J. Am. Chem. Soc.* **1943**, *65*, 2324).

(14) Jager, J. Ph.D. Thesis; University of Groningen, Groningen, The Netherlands, 1987.

(15) Unless otherwise stated, the measurements were performed at 25 °C.

(16) Bruggeman, D. A. G. *Ann. Phys.* **1935**, *24*, 636.

that effectively starts a polymer chain varies from 26% (solvent = 1,4-dioxane; atmosphere = air) to 10% (solvent = methyl ethyl ketone; atmosphere = N_2). These percentages have been calculated assuming that each initiator molecule defragments into two radicals.

Low-molecular-weight polymers have been synthesized using an (additional) hydrophobic chain transfer agent, dodecane thiol (RSH), so that polymers of structure RS-[poly(acrylic acid)]-H are formed as main product. As an example, reacting 5 g (69.4 mmol) of acrylic acid with 0.8 g (2.01 mmol) of dilauroyl peroxide and 0.5 g (2.27 mmol) of distilled $C_{12}H_{25}SH$ (Aldrich) in 50 mL of methyl ethyl ketone under a nitrogen atmosphere afforded a polymer having a polymerization degree of 47 (by NMR; vide infra).[13]

2. Characterization of Hydrophobically Single-End-capped Poly(sodium acrylate)s. The absence of monomer was established by ^{1}H NMR using the characteristic peaks for the acrylic hydrogens at ca. 6 ppm. We note the importance of pH in recording the NMR spectra. At pH 1, the peaks are broader and shifted upfield relative to a solution of pH 10. This is due to a conformational change of the polymer from a compact globule at low pH to a more extended coil at high pH.[14] All NMR spectra were therefore recorded at pH 10. The presence of small peaks at 3.2 and 3.6 ppm indicated that contamination of the product with methanol or 1,4-dioxane is at most 2 wt %.

The number-averaged degree of polymerization was determined using ^{1}H NMR spectroscopy by comparing the intensities of the NMR peaks corresponding to the terminal methyl group (from the initiator) at ca. 0.95 ppm and the polymer backbone −CH− at 2.2 ppm, respectively. In addition, size exclusion chromatography was employed to determine M_w and M_n.

3. Synthesis and Characterization of a Fluorescently Labeled Hydrophobically Single-endcapped poly(sodium acrylate). Fluorescein methacrylamide was synthesized according to the following procedure. A 100 mL round-bottomed flask was loaded with 0.18 g (0.53 mmol) of fluoresceinamine, isomer I (Aldrich), and 50 mL of methyl ethyl ketone (Merck, pro analysi). Triethylamine (100 μl; 0.72 mmol) (Janssen) and 100 μl (1.03 mmol) of methacryloyl chloride (Fluka) were subsequently added to the solution. The flask was covered with aluminum foil to exclude light which might initiate polymerization of methacryloyl chloride. The mixture was allowed to stand for 2 h at room temperature. A crystalline precipitate formed. This solid was triethylammonium chloride. The mixture was cooled to 4 °C for 2 h to allow the solid to crystallize further. The liquid was decanted, and this solution of fluorescein methacrylamide was used in the second (copolymerization) step without further purification or isolation of the product.

The solution of the fluorescently labeled monomer in methyl ethyl ketone was transferred into a 100 mL round-bottomed flask, and 2.5 g (34.7 mmol) of distilled acrylic acid and 1.21 g (2.84 mmol) of dilauroylperoxide were successively introduced. The copolymerization reaction was performed as described above. The workup procedure was extended by one precipitation step in *n*-pentane to remove all of the unreacted fluorescein (-methacrylamide). The molecular weight of the resulting polymer was 9000 (NMR).

4. Preparation of Dispersions of Lamellar Droplets. Two surfactants were used: the anionic surfactant *sec*-dodecylbenzenesulfonic acid (DoBS acid; Marlon AS-3, *ex* Hüls) and the nonionic surfactant $C_{13-15}EO_{\langle 7\rangle}$ (Synperonic A7, *ex* ICI). Sodium citrate and sodium hydroxide, used to neutralize the DoBS acid, were of analytical grade (Merck, pro analysi). The lamellar dispersions were prepared as follows. Twenty weight parts of electrolyte was added to 60 weight parts of water, together with NaOH (1.04 equiv, with respect to DoBS acid). DoBS-acid (the equivalent of 28 weight parts NaDoBS) and 12 weight parts of nonionic surfactant were added as a nonaqueous premix. After addition of each ingredient, the system was stirred until a homogeneous appearance of the mix was obtained or the solid ingredients were dissolved before the next ingredient was added. At the end of the process, the dispersion was stirred for at least 0.5 h.

The resulting dispersion of lamellar droplets is designated as a 40/60/20 model system (40 weight parts of surfactant, 60 parts of water, and 20 parts of electrolyte). Stabilizing polymer was added on top in quantities of 0.1−4% (w/w). Alternatively, to control the volume fraction of lamellar droplets (ϕ_{lam}), the polymer-free model system was allowed to phase-separate during two weeks, and a surfactant-rich lamellar phase (containing ca. 60% of surfactants by weight, $\phi_{lam} = 1$) separated from the isotropic continuous phase [containing only water and 30% (w/w) of sodium citrate·$2H_2O$]. Stabilizing polymer was added in 0.5−8% (w/w) to the surfactant-rich phase, and the thick mixture was homogenized by stirring and was allowed to stand for 1 week at 50 °C. By diluting this concentrated sterically stabilized dispersion with its own continuous phase, ϕ_{lam} was adjusted to any value between 0 and 1.

Methods. *1. General.*[15] NMR spectra were recorded at room temperature on a Varian Gemini (200 MHz) or Varian VXR300 (300 MHZ) instrument. A Philips PU 8740 UV/Vis spectrophotometer was employed to record UV/Vis absorption spectra. Viscosities of polymer solutions were determined using an Ubbelohde capillary viscometer, immersed in a water bath having a temperature of 30.0 ± 0.1 °C. The capillary tube was connected to a Schott AVS 400 automatic measuring system. 40/60/20 lamellar dispersions were phase-separated by centrifugation at 40 000 g for 2 h using a Beckman J2-21M/E centrifuge. Phase separation of dilute lamellar dispersions ($\phi_{lam} < 0.3$) or removal of entrapped air bubbles in concentrated lamellar dispersions ($\phi_{lam} > 0.8$) was accomplished by mild centrifugation (4000 g) using an AHT 5200 centrifuge.

2. Electron Microscopy. Electron micrographs of all samples were obtained by freeze-fracture−etching−heavy metal replication. 5 μl aliquots were physically fixed by slam-freezing using a Reichert MM80 immersion cryofixation system. The obtained frozen samples were fractured at −150 °C (Cressington CFE50) and etched at a temperature of −100 °C by vacuum sublimation for 2 min. A replica of the exposed surface was made having a 2 nm tungsten/tantalum layer thickness and a 7 nm carbon backing. Digital image acquisition was performed with a Gatan 694 slow-scan CCD camera.

3. Electrical Conductivity and Calculation of ϕ_{lam}. The volume fraction of the lamellar phase (ϕ_{lam}) was calculated from the electrical conductivity of the lamellar dispersion using the Bruggeman equation:[16]

$$\frac{\kappa - \kappa_{lam}}{\kappa_{el} - \kappa_{lam}} \cdot \left(\frac{\kappa_{el}}{\kappa}\right)^{1/3} = 1 - \phi_{lam} \qquad (1)$$

where κ denotes the electrical conductivity of the dispersion, κ_{lam} is the electrical conductivity of the lamellar droplets, and κ_{el} refers to the electrical conductivity of the continuous electrolyte phase. Electrical conductivity was measured using a Wayne-Kerr Autobalance Universal Bridge B642 fitted with a Philips PW9512/01 conductivity

cell having a cell constant of 1.5. If necessary, entrapped air bubbles were removed by mild centrifugation. κ_{lam} was found to be 0.7 mS/cm, which compares favorably with the literature value of 0.8 ± 0.2 mS/cm;[17] $\kappa_{el} = 61$ mS/cm.

4. Light Microscopy. Samples of lamellar dispersions were inspected with a Zeiss Axioplan light microscope, using polarized light. A small drop of material was placed on a microscope slide and quickly covered with a cover glass. Initially the sample flows to fill the gap between the slide and the cover glass; images were recorded after a few minutes, when the flow had almost stopped.

5. Size Exclusion Chromatography. Polymer molecular weights were determined by size exclusion chromatography. Polymer separation was performed using a sequential array of three columns (Biogel SEC 40XL, 30XL, and 20XL). The fractions were analyzed employing a Viscotek model 200 differential refractive index detector (to determine M_n) and a tri-angle laser light scattering detector (to determine M_w).[18]

6. MALDI−TOFSPEC. (Matrix-Assisted Laser Desorption and Ionization Time-of-Flight Mass Spectrometry). A drop of sample mixture containing 200 μl of a methanolic solution of 3.3 mg/mL ion-exchanged polymer (acid form) and 5 μl of 150 mM sodium acetate was put onto a matrix, consisting of α-cyano-4-hydroxy-cinnamic acid/acetone or 2,5-dihydroxybenzoic acid/acetone. A nitrogen laser was used to excite the matrix at 337 nm. The spectrometer employed was a Micromax TOFSPEC; the acceleration voltage was 20 kV.

7. X-ray Diffraction. Bilayer repeat distances in lamellar droplets were evaluated from X-ray diffractograms. A Kratky small-angle camera, equipped with a Braun PSD counter, was installed on a PW1729 generator with a copper anode (Cu Kα radiation) operated at 2 kW (50 kV, 40 mA).

8. Time-Resolved Fluorescence and Fluorescence Anisotropy. Fluorescence and fluorescence anisotropy decays were measured using the time-correlated single-photon-counting technique.[19] The fluorescent probe was excited at 460 nm with vertically polarized light. Erythrosin B served as a reference compound to yield the instrument response function. After excitation, the parallel and perpendicularly polarized fluorescence intensities were monitored using a 539.4 nm line filter (Schott, bandwidth 13.0 nm) in combination with a cutoff filter (Schott KV520). The decay curves were analyzed both by nonlinear least-squares fitting of the data with a sum of exponentials and by means of the maximum entropy method. For more details, we refer to relevant literature references.[20]

9. Fluorescence Correlation Spectroscopy. The fluorescence correlation spectroscopic (FCS) measurements were carried out using a Zeiss Evotec ConfoCorJ system using the 488 nm Ar ion laser line for excitation and the "fluorescein" emission filter set (maximum transmission between 530 and 570 nm). The principle and experimental realization of FCS have been outlined in several recent papers.[21] The autocorrelation curve was acquired during 20 s. The FCS data were analyzed with nonlinear least-squares fitting of the parameters in the autocorrelation function describing diffusion in a Gaussian volume element with radii ω_1 and ω_2 (e^{-2} intensity points of the Gaussian beam, the subscripts 1 and 2 refer to the equatorial and axial radius, respectively):

$$G(t) = 1 + \frac{1}{N}\left(\frac{1}{1+\frac{t}{\tau_d}}\right)\sqrt{\frac{1}{1+\frac{t}{a^2\tau_d}}} \qquad (2)$$

where N is the number of fluorescent molecules, a is equal to ω_1/ω_2, and τ_d is the diffusion time that is related to the translational diffusion constant D_{trans}:

$$D_{trans} = \frac{\omega_1^2}{4\tau_d} \qquad (3)$$

N and τ_d are the parameters to be recovered, while a was obtained by measuring the diffusion of an aqueous solution of 50 nM Rhodamine 6G under identical experimental conditions. Typical values are $\omega_1 = 0.246$ μm and $a = 7.0$.

10. Particle Sizing. Particle sizes were measured using a Malvern MasterSizer X Long Bed. The technique is based on the principle of laser ensemble light scattering (laser diffraction): particles scatter light so that the measured energy on the detector has a peak at a favored scattering angle that is related to the particle size. Over the size range 2 μm and upward, the scattering angle is largely independent of the optical properties of the material or the medium of suspension and is caused by diffraction of light around the particle. Light that couples into the particle is absorbed and can be ignored. However, in the case of smaller particles, the light coupled into a particle is not completely attenuated and can emerge as a refracted ray. This problem has been solved by using Mie theory, taking into account the optical properties of the sample.

The fundamental result measured by the instrument is a volume-weighted size distribution (d[4,3]), but the result may be transformed to surface- ([d[3,2]) or number- (d[1,0]) averaged weighings according to $X_i = V_i d_i^{T-3}$, where X_i is the relative frequency of the transformed distribution, V_i is the relative frequency of the volume distribution, d_i is the mean diameter of size class i, and T is 3 to transform to volume weighting, 2 for surface weighting, 1 for length, and 0 for number.

In a typical experiment, 1 drop of a concentrated lamellar dispersion was diluted into ca. 105 g (87.5 mL) of an aqueous solution containing 30% (w/w) trisodium citrate dihydrate; the average particle size was measured immediately. The following optical parameters were used: the refractive index (RI) of the lamellar droplets was calculated as 1.447 (vide infra),[22] the refractive index of the sodium citrate solution was determined to be 1.3840, and the imaginary reflective index of the lamellar droplets was found to equal to 0.15. The latter value was obtained by matching the actual (weighted-in) volume percentage of particles with the particle concentration calculated by the software.

(17) Van de Pas, J. C. *Tenside Surf. Det.* **1991**, *28*, 158.

(18) For basic principles, see: Brandrup, J.; Immergut, E. H. *Polymer Handbook*; 3rd ed.; Wiley: New York, 1989.

(19) Van Hoek, A.; Visser, A. J. W. G. *Proc. SPIE-Int. Soc. Opt. Eng.* **1992**, *1640*, 325.

(20) (a) Bastiaens, P. I. H.; Van Hoek, A.; Benen, J. A. E.; Brochon, J. C.; Visser, A. J. W. G. *Biophys. J.* **1992**, *63*, 839. (b) Leenders, R.; Kooijman, M.; Van Hoek, A.; Veeger, C.; Visser, A. J. W. G. *Eur. J. Biochem.* **1993**, *211*, 37.

(21) (a) Eigen, M.; Rigler, R. *Proc. Natl. Acad. Sci. U.S.A.* **1994**, *91*, 5740. (b) Rigler, R. *J. Biotechnology* **1995**, *41*, 177. (c) Thompson, N. L. In *Topics in Fluorescence Spectroscopy*; Lakowicz, J. R., Ed.; Plenum Press: New York, 1991; Vol. 1, pp. 337−378.

(22) The reported value corresponds to the refractive index of lamellar droplets present in a 40/60/20 model system containing 1% w/w of EC7800.

(23) Mohammadi, M. *Adv. Colloid Interface Sci.* **1995**, *62*, 17.

(24) Dispersions of lamellar droplets have low (volume fraction-dependent) viscous and elastic moduli, which provides strong evidence against the doubly endcapped nature of the stabilizing polymers, since this would result in bridging interactions. (Kevelam, J.; et al. *Langmuir* **1995**, *15*, 5002.

Scheme 2

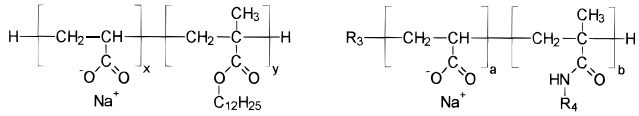

RAN4000: x/y = 25/1, MW = 4000

EC1000 - EC34000: a = 9-370, b = 0
FEC9000: a = 96, b = 0.5, R_4 = fluorescein
$R_3 = C_{11}H_{23}[CO_2]$ or $C_{12}H_{25}S$

Volume-averaged particle sizes of droplets in concentrated dispersions were determined using colloidal refractometry, which is an indirect method relating the measured refractive index of an undiluted dispersion (n) to an average particle diameter (d), using a general approximation of Mie theory:[23]

$$n = n_c + \phi(n_p - n_c)\frac{\sin x}{x} \quad x = \frac{4.5(n_p - n_c)d}{\lambda_0} \qquad (4)$$

where n_c and n_p denote the refractive indices of the medium and the particles; respectively, and λ_0 is the wavelength of light in a vacuum used in the measurement of n. Due to the turbidity of the dispersions, refractive indices were measured in reflection, using a Bellingham & Stanley RFM 91 multiscale automatic refractometer. The refractive indices of the lamellar droplets were calculated from the molar refractivities and volume fractions of the compounds comprising the lamellar phase.

11. Confocal Scanning Light Microscopy (CSLM). A BioRad MRC1024 CSLM, equipped with a Zeiss Axiovert 100 inverted microscope, was used to record CSLM images of lamellar droplets with anchored fluorescently labeled polymers. The fluorescein fluorophores were excited at 488 nm using an Ar/Kr mixed gas laser; the emitted light was detected at 522 ± 16 nm. An oil immersion objective (63X, N. A. = 1.25) was used to image the samples; the digital resolution was 512 × 512 pixels.

Results and Discussion

Synthesis of Hydrophobically Single-Endcapped Stabilizing Polymers. Well-defined steric stabilizers with a hydrophobic anchoring group at one terminus of the molecule have been synthesized in good yields (Scheme 2). The procedure is straightforward and versatile. The polymer nomenclature adopted is best illustrated by examples. EC1000 denotes a hydrophobically endcapped polymer having a number-averaged molecular weight of 1000; RAN4000 is a random copolymer of acrylic acid and lauryl methacrylate of molecular weight 4000 (this is the only "random" polymer that has been used in this study, just for comparative purposes; it contains 4 mol % of hydrophobes).

MALDI−TOFSPEC yields valuable insights into the nature of the polymer molecules with regard to their molecular weight and (most probable) structure. Thus, a poly(acrylic acid) that was synthesized in the presence of dodecyl thiol as a chain transfer agent was found to exist mainly as $C_{12}H_{25}S(CH_2CH_2CO_2H)_nH$; i.e., the polymer is endcapped. The fact that for the $[M-H]^+$ ion a major series was observed at $m/z = (417 \pm 1) + n(72 \pm 1)$ provides evidence for this statement (below $m/z = 417$, peaks from the matrix dominate the mass spectrum). Similar information provided evidence for the single-endcapped nature of a poly(acrylic acid) that was synthesized in the absence of a chain transfer agent. Indeed, from a rheological study of dispersions of lamellar droplets containing these polymers,[24] we have good indications for the hydrophobically single-endcapped nature of all the polymers under study. With this knowledge we could routinely determine number-averaged molecular weights using ^{1}H NMR by determination of end groups.[25] Since the method demands high accuracy of the integration of the NMR spectra, we checked the results using three independent techniques. First, we compared the molecular weight of a reference poly(acrylic acid), synthesized for this purpose using 1 mol % of AIBN, as determined by NMR and by viscosimetry. The viscosity-averaged molecular weight (M_v) was calculated as 51 500.[26] From NMR, the number-averaged molecular weight (M_n) was found to be 25 000. It is known that for polydisperse samples $M_n < M_v < M_w$.[27] Since M_w/M_n is typically 2−4 for this kind of polymers (Table 1), the obtained ratio of $M_v/M_n = 2$ is reasonable.

Table 1. Molecular Weights of Endcapped Poly(acrylates) As Determined by NMR and by SEC

polymer	M_w (SEC)	M_n (SEC)	M_n (NMR)	M_w/M_n (SEC)
EC750	605	360	750	1.8
EC1500	2 700	1 900	1 500	1.4
EC3000	4 300	3 100	3 000	1.4
EC8500	25 000	10 000	8 500	2.5
EC29000	82 000	27 000	29 000	3.0

Second, molecular weights of selected polymers were independently measured using size exclusion chromatography (SEC). The similarity between M_n as determined from NMR and SEC is satisfying (Table 1), providing good indications that these polymers are indeed endcapped.

Finally, for one low-molecular-weight polymer, we found good correspondence between $M_n = 750$ as determined by NMR and the peak of major intensity at $m/z = 635$ in the (MALDI) mass spectrum.

Synthesis and Properties of Fluorescently Labeled Hydrophobically Endcapped Stabilizing Polymers. Fluorescently labeled steric stabilizers FEC1000, FEC3000, and FEC9000 were synthesized with the aim to undertake a CSLM study of a dispersion of stabilized lamellar droplets. This would enable us to visually locate the stabilizing polymer, and thus to infer the stabilization mechanism. Such a study has been undertaken for fluorescently labeled RAN4000.[28]

UV/vis spectroscopy was employed to determine the amount of fluoresceinamine that had been incorporated into the polymers.[29] The extinction coefficient (ϵ) of free fluoresceinamine in water is 76.63×10^3 M^{-1} cm^{-1} at pH > 7.5 and is not affected by the presence of salt [30% (w/w) trisodium citrate dihydrate] or the presence of hydrophobically endcapped polymers up to at least 5% (w/w). From the absorbance at 488 nm of a polymer solution of known concentration, using the extinction coefficient of fluoresceinamine, it was calculated that, on average, 40% of the polymer molecules contained a fluorescent label.

It is of importance to establish with certainty the absence of fluorophore that is not covalently bound to the polymer. This is particularly obvious with regard to the interpretation of CSLM micrographs of lamellar droplets with added FEC9000 (see below). A way of establishing the absence of free fluoresceinamine in the polymer is to measure the fluorescence lifetimes of free and bound probes; we only

(25) (a) Bevington, J. C.; Ebdon, J. R.; Huckerby, T. N. In *NMR Spectroscopy of Polymers*; Ibbett, R. N., Ed.; Chapman & Hall: Glasgow, 1993. (b) Garmon, R. G. In *Polymer Molecular Weights, Part I*; Slade, E. P., Jr., Ed.; Marcel Dekker: New York, 1975.

(26) Newman, S.; Krigbaum, W. R.; Laugier, C.; Flory, P. J. *J. Polym. Sci.* **1954**, *14*, 451.

(27) Hiemenz, P. C. *Polymer Chemistry: The Basic Concepts*; Marcel Dekker: New York, 1984.

(28) Blonk, J. C. G.; Pas, J. C., van de; Visser, A.; Brouwn, L. F. *Colloids Surf. A* **1998**, *144*, 287.

(29) For UV/Vis absorption spectral data of fluoresceinamine, isomer I, see: *Sigma-Aldrich Library of Stains, Dyes and Indicators*; p 379.

describe the results obtained for FEC9000 (Table 2). The short lifetime of 17 ps of free fluoresceinamine could not be detected in the polymer sample, which provides hard evidence for the absence of free fluoresceinamine. Furthermore, the weighted average fluorescence lifetime of the polymer-bound fluorescent label is 185 times longer than that of free fluoresceinamine in solution. This is in agreement with the observation that the steady-state fluorescence intensity of polymer-bound label is much (ca. 100 times) larger than that of free fluoresceinamine. However, these results do not suggest the absence of free fluorescein methacrylamide since it is well-known that the chemical modification of the amino-functionality into an amide group is responsible for the fluorescence intensity enhancement.[30] We have not studied the photophysical origin of this effect.[31]

To determine with complete certainty that *all* fluorescent molecules are incorporated into the polymer, we studied the time-resolved fluorescence depolarization of free versus covalently bound fluoresceinamine. The results are summarized in Table 2. The average rotational correlation time for free fluoresceinamine is short, indicating a high degree of rotational freedom. For the polymer-bound fluorescent probe, the correlation time of 0.16 ns has disappeared completely, which indicates the absence of free probe molecules. A correlation time of 0.4 ns is present, providing evidence that one mode of internal rotation is not restricted by the polymer backbone. The presence of a long correlation time reflects rotation of the polymer as a whole.

Finally, we quantitatively describe the molecular dynamics of the fluorescently labeled polymer FEC9000. In general, the fluorescence anisotropy of a fluorophore incorporated into an irregularly shaped macromolecule, tumbling in solution, can be described by a sum of five exponential terms, which reduces to a triple exponential when there is certain (ellipsoidal) symmetry.[32] In practical cases, one measures a single harmonic mean correlation time characteristic of overall rotational tumbling;[33] when there are other sources of depolarization, as in our case, the anisotropy can be written as a Soleillet product of correlation functions:[34]

$$r(t) = (\beta_1 e^{-t/\chi_{internal}} + \beta_2) e^{-t/\chi_{overall}} \quad (5)$$

in which $\chi_{internal}$ is the time constant for internal motion of the fluorophore, $\chi_{overall}$ is the time constant corresponding to overall tumbling of the macromolecule, and $\beta_1 + \beta_2$ is the fundamental anisotropy. We can define a second-rank order parameter (S) for the fluorophore in the macromolecule:

$$S^2 = \frac{\beta_2}{\beta_1 + \beta_2} = \frac{1}{2}\cos\psi\,(\cos\psi + 1) \quad (6)$$

where ψ is the angular displacement of the fluorophore due to internal reorientation; $S = 1$ when there is no flexibility ($\beta_1 = 0$). The rate of reorientation is given by the diffusion coefficient ($D_\perp$) of internal motion:[35]

$$D_\perp = \frac{1 - S^2}{6\chi_{internal}} \quad (7)$$

Using $\chi_{internal} = 0.45$ ns, $\chi_{overall} = 4.59$ ns, $\beta_1 = 0.227$, and $\beta_2 = 0.095$, we obtain the following results: $S = 0.543$, $\psi = 65°$, $D_\perp = 2.63 \times 10^8\ s^{-1}$. Thus, the fluorescent label has appreciable internal mobility.

Table 2. Fluorescence Lifetimes (τ) and Rotational Correlation Times (ρ) of Free and Polymer-Bound Fluoresceinamine

	τ (ns)	α^a	ρ (ns)	β^b
free fluoresceinamine	0.017	0.99	0.16	0.44
			0.43	0.56
polymer-bound fluoresceinamine	0.427	0.15	0.41	0.53
	2.1	0.10	2.22	0.28
	3.9	0.73	15.5	0.08

[a] Relative occurrence or "amplitude" of lifetime. [b] Relative occurrence or amplitude of correlation time.

General Features of Lamellar Droplets with Added Endcapped Polymers. The first question to address is whether these hydrophobically endcapped polymers are capable of stabilizing the lamellar dispersion. Provided that the anchor density is kept constant, the stabilizing properties of all of the endcapped polymers under study, with molecular weights varying between 1000 and 30 000, appear to be comparable to those of the commercial random polymer.[36] Thus, 1.5 wt % of EC7800 suffices to turn an otherwise macro-phase-separated 40/60/20 model system into a homogeneous milky liquid, which is deflocculated on a microscopic scale.

A second question is related to the structural properties of the lamellar phase in the presence of anchoring endcapped polymers. The observation of Maltese crosses (Figure 1) provides evidence for the spherical nature of the particles. Freeze-fracture−etching electron microscopy corroborates this picture (Figure 2).

Finally, the bilayer repeat distance in the multilamellar vesicles is hardly affected by anchoring polymers, whether endcapped or having a random anchor distribution, as is shown in Table 3. Thus, the anchored steric stabilizers do not significantly affect the intralamellar forces. Moreover, the effect of ϕ_{lam} on the bilayer repeat distance is negligible.

Effect of the Amount of Adsorbed Polymer on Particle Size Studied by Laser Diffraction. Laser diffraction can be employed to establish particle size distributions in very dilute dispersions. This implies that a typical 40/60/20 model system has to be diluted approximately 7000-fold to obtain reliable results. To prevent swelling of the layers, the lamellar droplets are diluted into water containing 30% (w/w) of sodium citrate, as this solution closely resembles the continuous phase of the model system. However, although dilution of the surfactants may not cause problems, the concomitant dilution of the polymer will result in significant desorption from the lamellar droplets unless its affinity for the bilayer is very large.

As a critical test of the method, we diluted 1 drop (0.014 g) of 40/60/20 model system containing 1% (w/w) of EC7800 into 105 g (87.5 mL) of an aqueous solution containing 30% (w/w) of trisodium citrate dihydrate; the average

(30) Rypacek, F.; Drobnik, J.; Kalal, J. *Anal. Biochem.* **1980**, *104*, 141.

(31) One possibility is that the nonbonded electron pair on the (amino-) nitrogen atom in fluoresceinamine quenches the fluorescence of the molecule through photoelectron transfer (cf. Bissell, R. A.; Prasanna da Silva, A.; Gimal Gunaratne, H. Q.; Mark Lynch, P. L.; Maguire, G. E. M.; Samankumara, K. R. A. *Chem. Soc. Rev.* **1992**, 187). In case of fluoresceinmethacrylamide, the elecron pair will be partly delocalized into the carbonyl group, which reduces the efficiency of quenching.

(32) Small, E. W.; Isenberg, I. *Biopolymers* **1977**, *16*, 1907.

(33) Berkhout, T. A.; Visser, A. J. W. G.; Wirtz, K. W. A. *Biochemistry* **1984**, *23*, 1505.

(34) Bastiaens, P. I. H.; Van Hoek, A.; Wolkers, W. F.; Brochon, J. C.; Visser, A. J. W. G. *Biochemistry* **1992**, *31*, 7050.

(35) Szabo, A. *J. Chem. Phys.* **1984**, *81*, 150.

(36) Qualitative information obtained from stability studies of complete liquid detergent formulations (unpublished results).

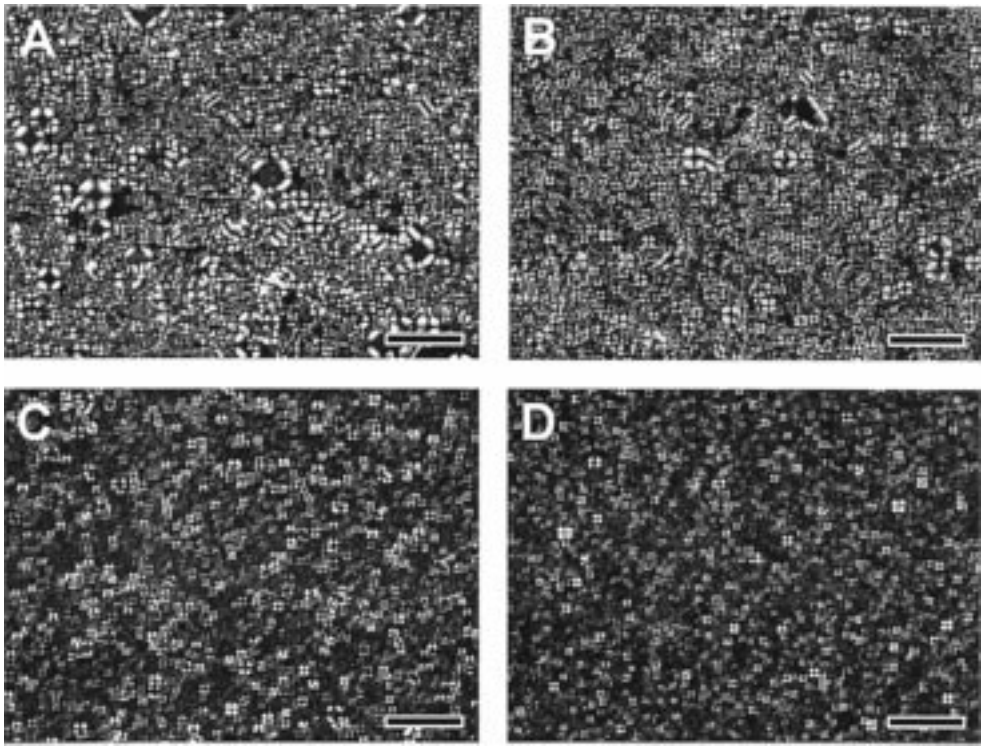

Figure 1. Light micrographs of a concentrated dispersion of lamellar droplets ($\phi_{lam} \approx 0.7$) showing the influence of the molecular weight of the stabilizing polymer on the average droplet size. The molecular weight increases from left top to right bottom: EC3000 (A), EC7800 (B), EC19000 (C), and EC34000 (D). Magnification is 40X; bar indicates 5 μm.

particle size was measured immediately ($t = 0$) and then as a function of time. Microliter aliquots of a concentrated solution of EC7800 were subsequently added, and the particle size was measured again at different time intervals. From Table 4, it appears that the average particle size increases in time after dilution of the 40/60/20 model system with citrate solution. This process is reversible; d[3,2] is decreased as stabilizing polymer is added to the dilute dispersion. Moreover, adding more and more polymer results in a size reduction of the largest droplets, as evidenced by a decrease of the volume-averaged particle size d[4,3].

Thus, the size (but not the shape) of the deformable membranes *responds* to the presence of the adsorbed polymer chains. It is convincingly demonstrated that increasing the amount of adsorbed polymer (at constant molecular weight) results in a decrease of the particle size. A likely interpretation considers the lateral tension in the system as the dominant factor. Particularly in the brush regime, where energy is stored in the adsorbed polymer, increasing the local density of polymer segments near the particle surface will result in an increased lateral tension in the polymer layer; this tension can be relaxed by increasing the curvature of the particle, i.e., by decreasing the particle size.[37]

Finally, these processes take place in a time scale of minutes (adsorption being faster than desorption, indicating a larger-than-unity binding constant; vide infra). This has important implications for the application of laser diffraction to determine particle sizes of self-assembled lamellar droplets; the measurements are reliable only if taken immediately after the dilution step.

Droplet Size in Concentrated Dispersions: The Effect of the Amount of Adsorbed Polymer and of Polymer Molecular Weight. The average particle size of lamellar droplets in concentrated dispersions can be estimated from the volume fractions and molar refractivities of the individual components of the dispersion, in relation to the volume fraction and refractive index of the whole dispersion, using Mie theory (see Experimental Section). This approach eliminates the need for dilution of the sample.

We note that d[4,3] as determined by refractive index measurements is structurally lower than the value obtained from laser diffraction (Figures 5 and 6). This is most likely due to the fact that particles with a diameter exceeding 6 μm cannot be detected using colloidal refractometry. We contend that the observed trends can be taken to be reliable if the two techniques provide similar results.

The effect of the amount of polymer EC7800 added to a 40/60/20 system on the average particle size is depicted in Figure 3. At polymer concentrations below 1% (w/w) the particle size decreases rapidly with increasing polymer concentration. This result corroborates the previous finding (using a different technique) that increasing the grafting density results in an increased lateral tension in the adsorbed polymer layer, leading to a reduction in particle size.

However, if the grafting density increases, the particle size decreases less steeply with increasing polymer concentration. As we shall see below, this effect can at least partly be explained by the fact that polymer adsorption to the lamellar droplets becomes increasingly disfavored as the polymer concentration is raised beyond 1% (w/w).

As evidenced from the data in Figure 4, the average droplet size decreases steadily with increasing polymer molecular weight (at constant anchor density). This result is in line with the decrease of particle size with increasing polymer concentration (at constant molecular weight), and we contend that the same general principle underlies the

(37) Hristova, K.; Needham, D. In *Stealth Liposomes*; Lasic, D. D., Martin, F., Eds., CRC Press: Boca Raton, FL, 1995; p 44.

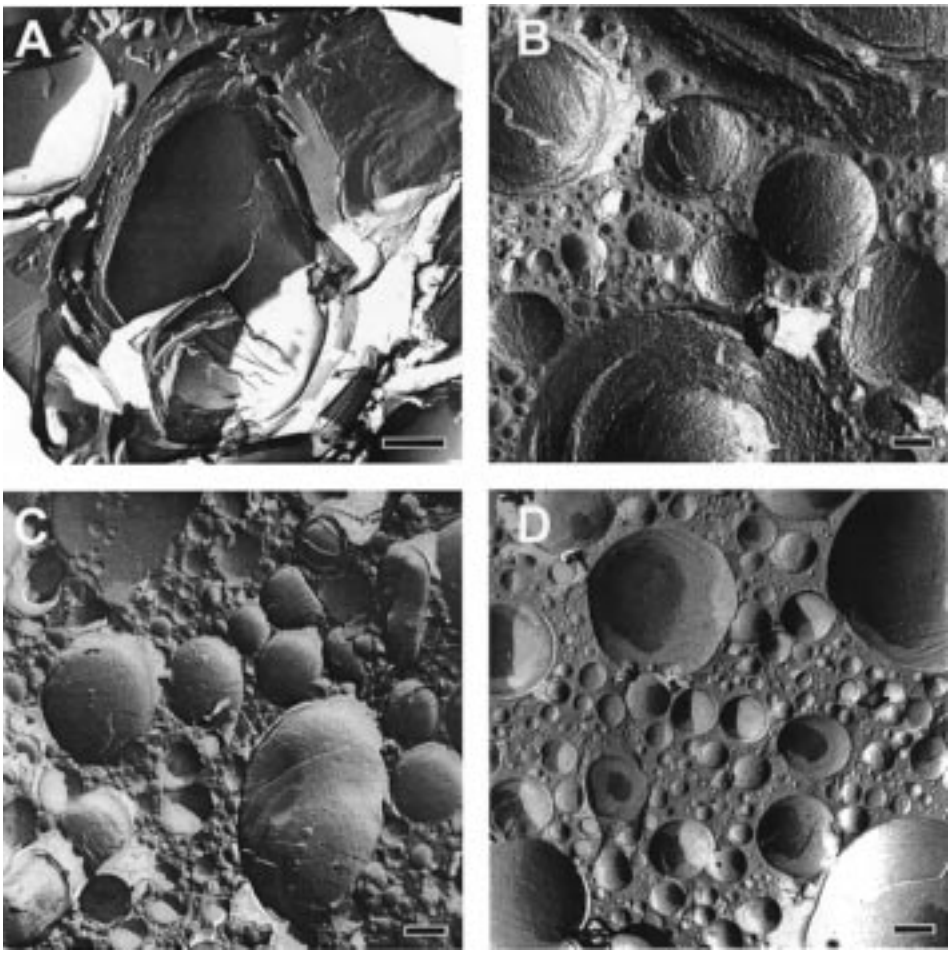

Figure 2. Freeze-fracture−etching electron micrographs of concentrated dispersions of lamellar droplets ($\phi_{lam} \approx 0.7$) with added EC1000 (A), EC3000 (B), EC19000 (C), and EC34000 (D). Bar represents 1 μm.

Table 3. Bilayer Repeat Distance in Lamellar Droplets with Anchored Poly(sodium acrylate)s as a Function of ϕ_{lam} and Polymer Molecular Weight

polymer	[polymer][a] (% w/w)	[surfactants] (% w/w)	ϕ_{lam}	bilayer repeat distance (nm)
none	none	60−63	1	3.30−3.40
EC1000	0.23	60.5	0.91	3.43
EC1000	0.21	55.8	0.85	3.45
EC1000	0.18	48.4	0.77	3.47
EC1000	0.17	45.5	0.72	3.44
EC3000	0.68	60.2	0.92	3.40
EC3000	0.51	45.3	0.73	3.43
RAN4000	0.91	60.1	0.92	3.42
RAN4000	0.68	45.2	0.73	3.44
EC7800	1.82	59.5	0.91	3.34
EC7800	1.37	44.8	0.76	3.42
EC19000	3.99	53.6	0.84	3.29
EC19000	3.47	46.5	0.78	3.32
EC19000	3.26	43.7	0.72	3.36
EC34000	6.00	42.3	0.65	3.30

[a] The polymer concentrations have been chosen such that the number of hydrophobic anchors per gram surfactant is constant. Thus, for a 40/60/20 model system, where the surfactant concentration is 30.33% (w/w) and $\phi_{lam} \approx 0.5$, [polymer]/% (w/w) = 0.12 (EC1000), 0.34 (EC3000), 0.46 (RAN4000), 0.91 (EC7800), 2.17 (EC19000), and 3.99 (EC34000).

two phenomena: the minimization of lateral repulsive forces between adsorbed polymer molecules. In other words, the adsorbed polymers need a larger "parking area" as the molecular weight of the backbone increases; the droplets react by decreasing their size as to increase the specific surface area.

Table 4. Time-Dependent Polymer Adsorption to and Desorption from Lamellar Droplets Studied by a Simple Dilution Experiment Using Laser Diffraction[a]

added [polymer] (%w/w)[b]	time (min)[c]	d[4,3] (μm)[d]	d[3,2] (μm)[e]
0	0	4.91	2.5
0	3	7.93	3.95
0	8	9.63	4.57
0.00286	1	6.07	2.8
0.00286	5	4.92	2.5
0.0143	1	4.3	2.43
0.0143	5	3.94	2.47
0.0876	1	3.73	2.54
0.0876	5	3.71	2.77

[a] For details with regard to the procedure, see text. [b] Concentration of added polymer in weight percent with respect to the total amount of diluted dispersion. The first addition of polymer (0.00286%) corresponds to 20 wt % with respect to the amount of model system present in the total amount of dispersion. [c] Time indicates time after addition of the model system to the aqueous citrate solution (first three entries) or time after addition of a certain amount of polymer to the dilute dispersion of model system (all following entries). [d] Volume-averaged particle size (maximum emphasis on largest droplets). [e] Surface area-averaged droplet size (less emphasis on large droplets).

Finally, we have studied the effect of ϕ_{lam} on d[4,3]. The results are summarized in Figure 5, and indicate that the largest particles become smaller with increased close-packing of the droplets.

Polymer Adsorption Isotherms. From the laser diffraction experiments (vide supra), it is clear that endcapped stabilizing polymers do not anchor into the

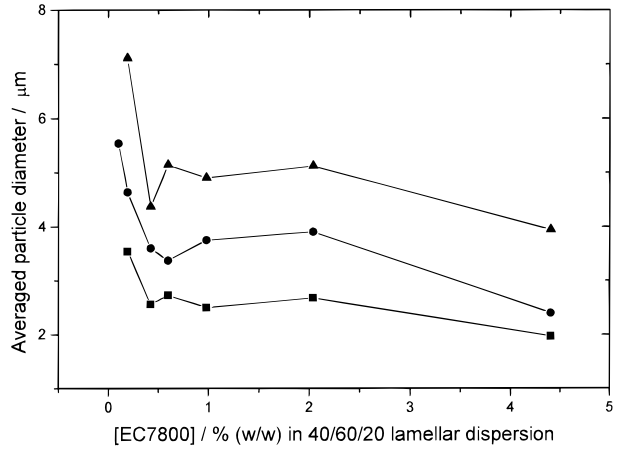

Figure 3. Volume- and surface-averaged particle size (d[4,3] and d[3,2]) determined by laser diffraction (LD) and refractive index measurements (RI) of lamellar droplets in a 40/60/20 model system as a function of the concentration of added stabilizing polymer EC7800. ▲ d[4,3] (LD); ● d[4,3] (RI); ■ d[3,2] (LD).

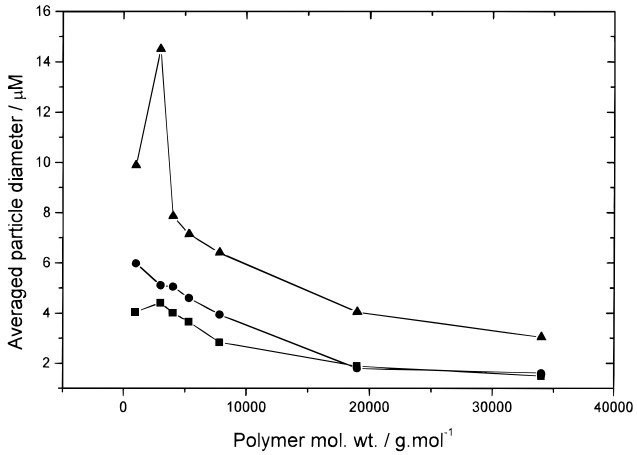

Figure 4. Volume- and surface-averaged particle size (d[4,3] and d[3,2]) of lamellar droplets in a 40/60/20 model system as a function of the molecular weight of added hydrophobically endcapped stabilizing polymer. ▲ d[4,3] (LD); ● d[4,3] (RI); ■ d[3,2] (LD).

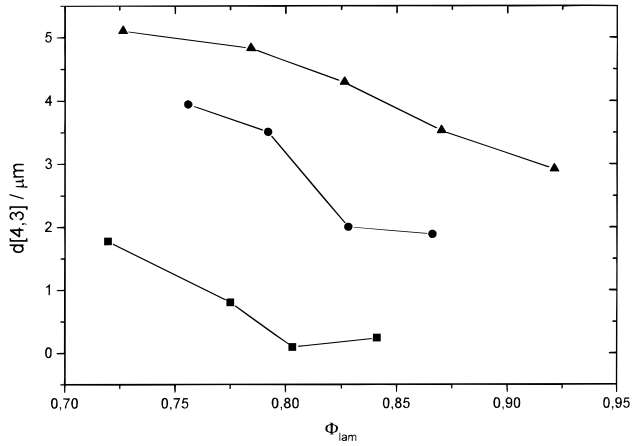

Figure 5. Volume-averaged particle size of lamellar droplets as a function of the volume fraction of lamellar phase as determined by refractive index measurements. ▲ EC3000; ● EC7800; ■ EC19000.

lamellar phase with an infinitely large affinity, and together with the observation that the amount of polymer adsorbed on the lamellar droplets determines their particle size, an important issue now involves a quantitative determination of the partitioning equilibrium or adsorption isotherm.

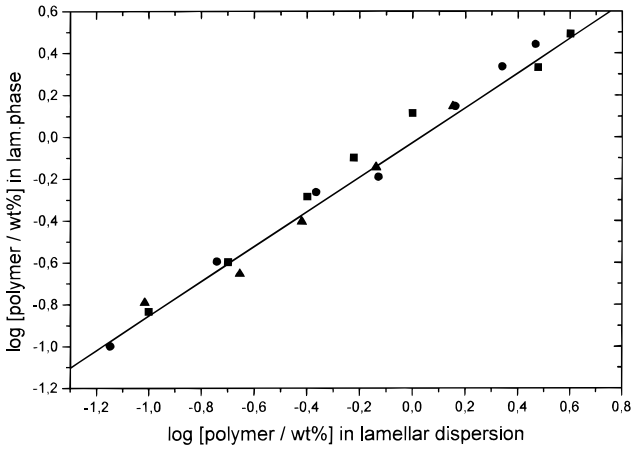

Figure 6. Adsorption of fluorescently labelled hydrophobically endcapped polymers to lamellar droplets in a 40/60/20 model system. The data have been fitted to a modified Freundlich isotherm, relating the adsorbed amount (w) to the total concentration of polymer in the model system (c'); for clarity, only the fit to the FEC1000 data is shown (grey line). ▲ FEC1000; ● FEC3000; ■ FEC9000.

We have tackled this problem by the use of hydrophobically endcapped poly(sodium acrylate)s covalently labeled with a dye (fluoresceinamine), FEC1000, FEC3000, and FEC9000. These polymers can be used to prepare sterically stabilized 40/60/20 model systems, which are not close-packed, so that the systems can be separated into a continuous phase and a lamellar phase by centrifugation. The continuous phase is analyzed for dye content by UV/Vis spectroscopy, and by applying a mass balance, the concentrations of polymer in the two-phase system can be calculated. In this way, we studied the adsorption of hydrophobically endcapped poly(sodium acrylate)s to the lamellar droplets in a 40/60/20 system at constant concentration of surfactants, as a function of polymer concentration and molecular weight. Adsorption data for all three polymers are depicted in Figure 6.

It is clear that if the concentration of polymer in the dispersion is increased, the amount of polymer adsorbed onto the lamellar droplets degressively increases. Moreover, at polymer input concentrations smaller than approximately 1%, the lamellar phase is enriched in polymer, whereas at higher concentrations, the amount of polymer associated with the lamellar phase is lower than that put into the model system. Thus, polymer adsorption becomes energetically less favorable with increasing polymer concentration. This finding is consistent with the notion that increasing the graft density at the surface results in an increased lateral tension within the polymer layer, the same factor that is held responsible for the concomitant reduction of the average particle size.

It appears that we can describe these adsorption phenomena in terms of a Freundlich isotherm, which represents the relation between the amount of a substance adsorbed to a nondeformable solid and the concentration of the substance in a solvent in contact with the solid:

$$w = kc^{1/a} \tag{8}$$

where w is the weight of material (in gram) adsorbed per gram of adsorbing solid, c is the concentration in solution at equilibrium (in gram/liter), and k and a are constants.[38]

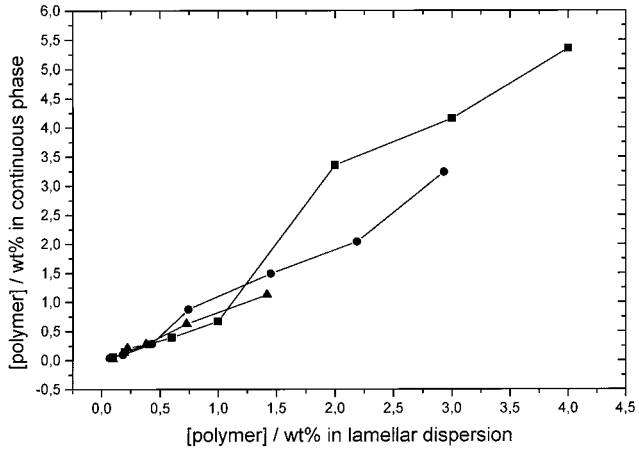

Figure 7. Polymer concentration in the continuous phase as a function of polymer concentration in a 40/60/20 model system. ▲ FEC1000; ● FEC3000; ■ FEC9000.

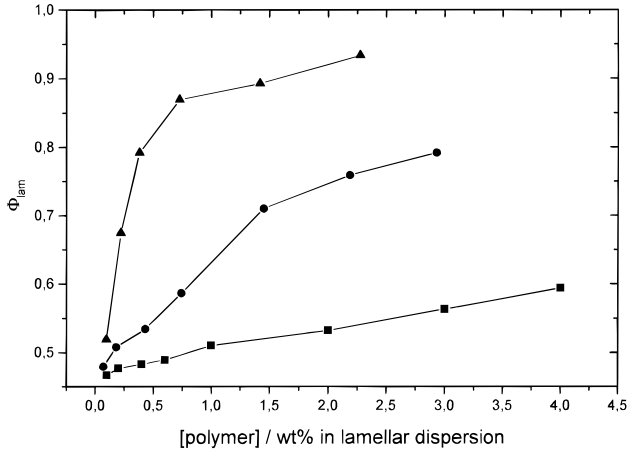

Figure 8. Volume fraction of lamellar phase (at constant surfactant concentration) as a function of polymer concentration in a 40/60/20 model system. ▲ FEC1000; ● FEC3000; ■ FEC9000.

For convenience, we use weight percentages instead of concentrations.

A slightly better fit is obtained when the amount of adsorbed polymer is correlated with the concentration of polymer put into the model dispersion ("modified" Freundlich isotherm).[39] The numerical value of constant a is 1.21 for EC1000, 1.15 for EC3000, and 1.22 for EC9000. This reflects the degressive increase of the amount adsorbed with the concentration of polymer in the dispersion. The fact that $k = 1$ for all three polymers corresponds to the "critical" polymer concentration of 1% mentioned above, where the concentration of free polymer exactly equals the concentration of adsorbed polymer.

Perhaps the most striking observation is the close agreement of the adsorption data for FEC1000, FEC3000, and FEC9000. One would expect that, for hydrophobically single-endcapped polymers, adsorption efficiency should increase with decreasing molecular weight; the hydrophilic coils occupy less space, and more polymers can adsorb before they start to repel each other at the surface of the droplets. Indeed, we find that the polymer concentration in the continuous phase increases with polymer molecular weight, which is consistent with the interpretation mentioned above (Figure 7). The analysis of the lamellar phase seems to be in contradiction with the analysis of the continuous phase.

We now encounter the limitations of the use of the Freundlich isotherm to describe a system where the substrate is not a hard surface. The lamellar droplets respond to the presence of the polymers. One important contribution is due to "building-in", i.e., the polymers FEC1000 and FEC3000 penetrating between the layers of the lamellar droplets. The strong increase of ϕ_{lam} with polymer concentration for FEC1000 and, to a lesser extent, FEC3000 points at the occurrence of this effect (Figure 8). FEC9000 appears to remain "outside" the droplets. Thus, the lamellar droplets can indeed accommodate more low-molecular-weight polymers than their high-molecular-weight counterparts, but the extra polymeric material is partly stored in the interior of the droplets, and the "intrinsic affinity" of low-molecular-weight material appears to be similar to that of high-molecular weight-polymers (Freundlich isotherm).

Another explanation for the invariance of the apparent adsorption behavior of the three polymers invokes a change of the properties of the continuous phase with polymer concentration and differently so in going from FEC1000 to FEC3000 to FEC9000. More specifically, we contend that at higher polymer concentrations mixed polymer/surfactant aggregates form in the continuous phase. For example, if the concentration of FEC9000 in a 40/60/20 model system exceeds 0.5% (w/w), mild centrifugation (at a few 1000g) is insufficient to obtain complete phase separation, that is, the continuous phase retains some turbidity. Thus, very small,[40] colloidally stable particles are formed above a polymer concentration of 0.5% (w/w). Using fluorescence correlation spectroscopy we showed that these particles are indeed coated by polymers: the translational diffusion time (τ_d) of the fluorescently labeled polymer FEC9000 in the presence of these particles is much larger than that in an aqueous citrate solution. For the "free" polymer (10 nM FEC9000 in 30% (w/w) trisodium citrate dihydrate), $\tau_d = 400\ \mu$s ($D_{trans} = 3.8 \times 10^{-11}$ m^2 s^{-1}), whereas for anchored polymers $\tau_d = 5$ ms ($D_{trans} = 3.0 \times 10^{-12}$ m^2 s^{-1}), indicating that these polymer molecules are involved in "large" aggregates which cannot be polymeric micelles since the polymer concentration is lower than its critical micelle concentration (cmc).[41] Therefore, the polymers have to be adsorbed on the surface of the small vesicles. Even if the lamellar dispersions are centrifuged at 40 000g until an optically clear continuous phase is obtained, this "isotropic" phase still contains appreciable amounts of (anionic) surfactant. As appears from Figure 9, surfactant levels in this continuous phase increase with polymer concentration.

It is clear that, at constant polymer concentration, surfactant levels in the continuous phase increase with decreasing polymer molecular weight. The explanation is that concentrations are reported in weight percentages: at a constant weight fraction of polymer in the sample, the number of polymer molecules, and therefore the

(38) Daniels, F.; Williams, J. W.; Bender, P.; Alberty, R. A.; Cornwell, C. D. *Experimental Physical Chemistry*; McGraw-Hill, Inc.: New York, 1962; pp 328−332.

(39) We stress that the use of the Freundlich isotherm to describe the adsorption of these polymers to lamellar droplets may not be justified theoretically since the surface area of the droplets is not constant; however, we accept the Freundlich equation as an empirical relationship to predict the amount of adsorbed polymer from the concentration of polymer in the dispersion, which is very convenient from a practical point of view.

(40) Since the solution is turbid, the diameter of the particles is on the order of the wavelength of visible light (a few hundred nm).

(41) The CMC of a hydrophobically endcapped polymer of $M_w = 8000$, in 30% w/w NaCit, is about 1 mM (to be published). The polymer concentration in the continuous phase is only 0.25% ≃ 2.5 g/L ≃ (2.5/8000) mol/L ≃ 0.3 mM (the continuous phase has been diluted after the centrifugation step).

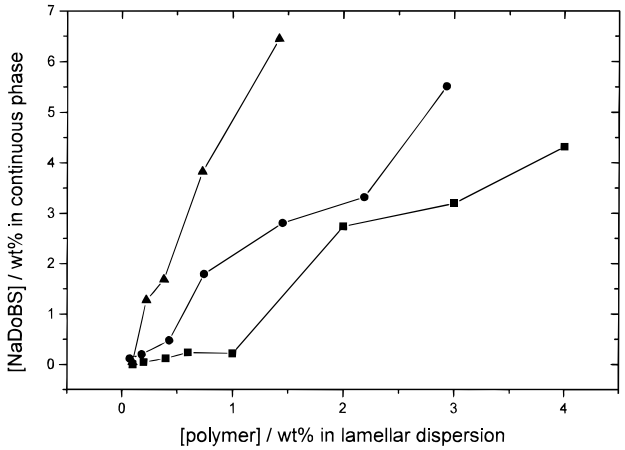

Figure 9. Concentration of anionic surfactant in the continuous phase as a function of polymer concentration in a 40/60/20 model system. ▲ FEC1000; ● FEC3000; ■ FEC9000.

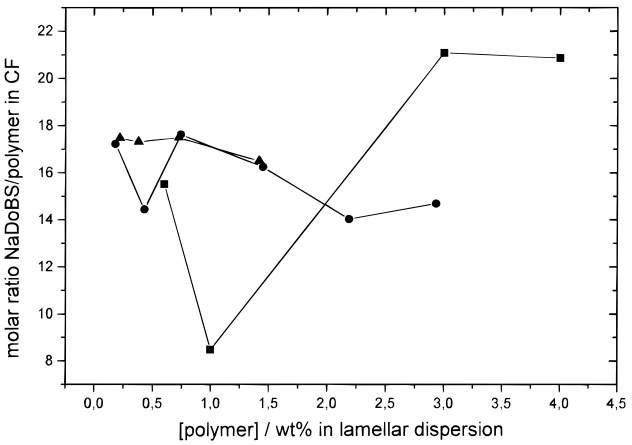

Figure 10. Composition of mixed aggregates (present in continuous phase) as a function of polymer concentration in a 40/60/20 model system. ▲ FEC1000; ● FEC3000; ■ FEC9000.

"solubilization capacity" for surfactant molecules, increases with decreasing polymer molecular weight. Indeed, as is shown in Figure 10, the *number* of surfactant molecules per polymer molecule in the mixed aggregates is relatively invariant with polymer molecular weight (error margins are large due to the fact that the polymer/surfactant ratio is obtained by division of two small numbers).

The polymer/surfactant ratio in the aggregates is, on average, $^1/_{18}$. As was shown by transmission electron microscopy (Figure 11), for FEC9000 concentrations exceeding 1 wt %, these aggregates comprise small (polymer-coated) vesicles (100 nm diameter).

Addition of polymer may break down the lamellar phase to some extent, resulting in the formation of polymer/surfactant mixed micelles.[42] However, in the concentration regime employed ($0 <$ [polymer]/wt % < 5) the main effect appears to reduce the average size of the lamellar droplets to form polymer-coated vesicles which are so small that they are colloidally dispersed in the continuous phase. The lower the polymer molecular weight, the larger the concentration of polymer and surfactant in the continuous phase, and the larger the concentration of polymer-coated small vesicles (or mixed micelles). This observation explains the apparent invariance of adsorption behavior

(42) Micelles cannot be observed by TEM if the negative staining technique is used; however, this does not imply the complete absence of micellar structures in solution.

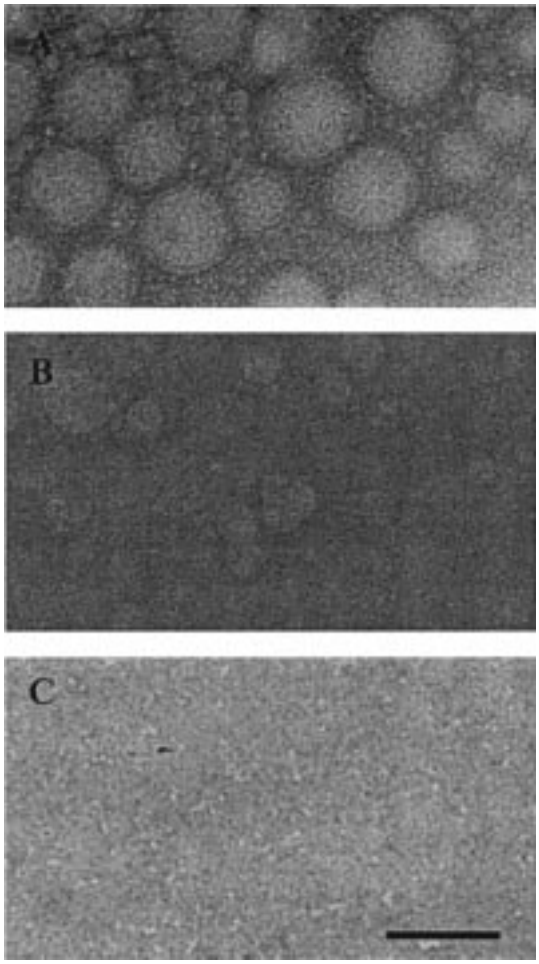

Figure 11. Transmission electron micrographs (negative staining, potassium tungstate) of (A) the continuous phase of a 40/60/20 model system containing 1 wt % of EC7800, (B) a solution of 1 wt % of EC7800 in an aqueous solution mimicking a continuous phase (i.e., containing 30 wt % of trisodium citrate·$2H_2O$), and (C) the continuous phase of a 40/60/20 model containing 0.25 wt % of EC7800. Bar represents 100 nm.

with molecular weight: low-molecular-weight polymers do adsorb to surfactant aggregates more efficiently than their higher-molecular-weight counterparts, but the size of some of these aggregates is too small to be comprised by the lamellar phase, and therefore, these adsorption processes cannot be detected. As a matter of fact, this issue validates a reconsideration of the definition of the continuous phase. One might argue that small, polymer-coated vesicles do not belong to the continuous phase but that they form the smallest lamellar structures comprised by the lamellar phase, whereas mixed micellar structures do belong to the continuous phase.

Finally, in another adsorption experiment, we diluted a 40/60/20 model system containing 2% (w/w) of FEC9000 with its own continuous phase and monitored the distribution of the polymer over the continuous and lamellar phase as described above. The results are depicted in Figure 12. It is surprising that the amount of adsorbed polymer is relatively invariant with the dilution factor (which is calculated as the mass of the 40/60/20 model dispersion divided by the total mass of dispersion plus added continuous phase). As the model system is diluted, the affinity of the polymer for the lamellar phase (as expressed by a partition coefficient $P = [\text{polymer}]_{\text{adsorbed}}/[\text{polymer}]_{\text{free}}$) increases rapidly, such that significant polymer desorption is prevented.

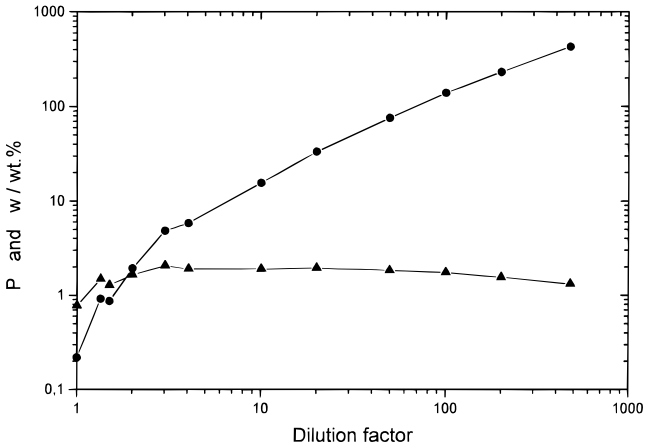

Figure 12. Partition coefficient for the distribution of polymer among the continuous and lamellar phase in a 40/60/20 model system (*P*; see text) and the amount adsorbed (*w*), as a function of the dilution factor. ▲ Adsorbed amount (w); ● partition coefficient (*P*).

On the basis of a chemical equilibrium of a polymer being distributed among two phases, one would expect that increasing the amount of the continuous phase would result in a decreasing amount of adsorbed polymer. This is not observed experimentally, and we attribute this to an opposing effect described by Gibbs' adsorption equation. Thus, if the adsorbed molecules keep the surfaces apart (as in steric stabilization), increasing the particle surface-to-surface separation (by diluting the dispersion) causes the amount of adsorbed substance to increase.[43]

Visualizing Steric Stabilization. We have seen that some of the lamellar droplets are so large that they can be observed using light in the visible wavelength region. The fact that the polymers have a covalently linked fluorescent dye provides a unique opportunity of literally visualizing steric stabilization using CSLM. This technique provides a view of a thin slice of the sample, where only fluorescent material can be observed.

Figure 13a shows a CSLM image of a 40/60/20 model system with 0.25% (w/w) of added FEC9000. The interiors of the droplets appear as dark spots; the area between the droplets shows fluorescence. This indicates that, according to expectation, the stabilizing polymers do not penetrate into the droplets. The explanation that fluorescence is observed throughout the continuous phase, and not exclusively at the rim of the droplets, lies in the fact that the polymer distributes itself among the lamellar and the continuous phase. If this sample is diluted with continuous phase, the concentration of free polymer is reduced (see above) and a clear, brightly fluorescent rim around the droplets becomes visible (Figure 13b). This is the polymer layer that is responsible for the steric stabilization.

Conclusions

The hydrophobically endcapped poly(sodium acrylate)s described in this study stabilize colloidal dispersions of lamellar droplets in concentrated aqueous salt solutions. The presence of an adsorbed polymer layer has been directly imaged using confocal scanning laser microscopy, which convincingly demonstrates that steric repulsion between adsorbed polymers is responsible for the colloidal stability of the droplets.

Of considerable importance for any study of flexible, deformable, sterically stabilized membranes is the following general conclusion. The amount of adsorbed polymer and the average droplet size are strongly interrelated through the lateral tension in the adsorbed layer. Thus, by increasing the amount of polymer adsorbed onto the lamellar droplets, the lateral tension in the droplets increases, and as a consequence, the average droplet size decreases and the propensity for anchoring is decreased.

(43) Everett, D. H. *Basic Principles of Colloid Science*; Royal Society of Chemistry: Letchworth, U. K., 1988.

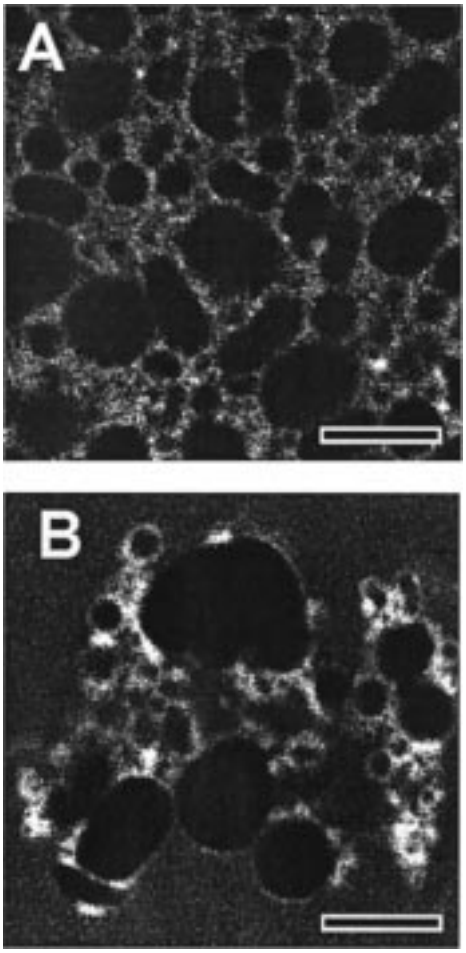

Figure 13. (A) CSLM image of lamellar droplets in a 40/60/20 system with added 0.25% (w/w) FEC9000 and (B) CSLM image of lamellar droplets in a 40/60/20 system with added 0.25% (w/w) FEC9000 after 30-fold (v/v) dilution with continuous phase. The apparent flocculated state of the droplets is due to creaming. The droplets occupy only a small volume fraction, so that they move rapidly upward under the influence of gravity. Within a minute, most of the particles have reached the top of the cell, where they are pushed against the cover glass.

Acknowledgment. Dr. J. M. Pestman is kindly acknowledged for skillfully preparing and examining negatively stained samples by electron microscopy. We gratefully thank W. M. du Chatinier for SEC analyses, E.C. Roijers for X-ray diffraction measurements, Drs. M. Paques, M. Leunis, and R. den Adel for recording the cryo-fracture electron micrographs, and Dr. P. J. W. Schuyl, G. A. Buijs, and J. J. Schilt for the MALDI−TOFSPEC analyses of EC750 and EC7800.

Appendix

Surface Occupancy of Lamellar Droplets by Decoupling Polymers. In this appendix, we evaluate the consistency of the obtained microstructural results in terms of a model in which the average particle size is directly related to the number and molecular weight of

the adsorbed polymer through the equation of the "parking area" of the polymer with the specific surface area of the droplets.

The area occupied by one decoupling polymer (A_p) depends on its gyration radius (r_0) by $A_p = \pi r_0^2$. The specific surface area (σ_d) of the lamellar droplets is related to the surface-averaged particle diameter and the density of the dispersion (ρ_d): $\sigma_d = 6/\{d[3,2]\cdot\rho_d\}$.

For 40/60/20 model systems with 1% (w/w) of added EC7800 we have determined $d[3,2] = 2.83\ \mu m$, so that the specific surface area $\sigma_d = 2\ m^2/g$ ($\rho_d = 1.15$). The concentration of EC7800 in the lamellar phase is approximately 1 wt %.

In other words, 1 gram of lamellar droplet has a surface of 2 m^2, which is covered by 0.01 g of polymer, or 1.28 μmol, or 7.7×10^{17} polymer molecules. Therefore, the surface area occupied per polymer molecule, required for stabilization, is $2.6 \times 10^{-18}\ m^2$. The polymer molecule, on the basis of its gyration radius, could have occupied $7.1 \times 10^{-18}\ m^2$ at least (for $r_0 = 1.5$ nm) and $137 \times 10^{-18}\ m^2$ at most (for $r_0 = 6.6$ nm). Thus, the polymer occupies the total surface area of the lamellar droplet and is even compressed.

In conclusion, by equating the total area occupied by the adsorbed polymer to the specific surface area of the particles, a direct link has been made between the amount and molecular weight of the adsorbed polymer and the average particle size. Moreover, the results suggest that EC7800 is adsorbed in the form of "brushes" rather than "mushrooms".

LA981636V